Planck 2015 Cosmological Results

Daniela Paoletti[1,2]
on behalf of the Planck Collaboration

[1]INAF/IASF-Bologna, via Gobetti 101, I-40129, Bologna, Italy
[2]INFN-Sezione di Bologna, viale Berti Pichat 6/2, 40127 Bologna, Italy

The *Planck* satellite has observed the full sky at nine frequencies between 30 GHz and 1 THz from 2009 to 2013. It represents the third generation of satellites dedicated to the observation of the Cosmic Microwave Background radiation (CMB). The CMB anisotropies represent the picture of primordial cosmological perturbations that originated the present structures of the Universe and *Planck* has performed their measurement with unprecedented accuracy in both temperature and polarization. In 2015 the *Planck* full mission data and results have been released to the public , here we will present some of the main cosmological results.

1 Introduction

The Cosmic Microwave Background (CMB) radiation is one of the most important source of information on the Universe origin, history, present and future status. It is the relic radiation from the Big Bang and it encodes the status of cosmological perturbations before stars and structures were formed. It was generated when the universe was cool enough to allow the recombination of neutral hydrogen (during the phase called *recombination*), increasing the mean free path of photons to lenghts of the order of the Universe size. The CMB represents the first picture of the Universe just 400000 years after the Big Bang and its photons were emitted from an hypothetical surface called the *Last Scattering Surface* (LSS). The CMB is almost perfectly isotropic in the sky with a blackbody spectrum at a temperature of T=2.72548 ± 0.00057 K [1], the small anisotropies of the order of $\Delta T/T \sim 10^{-5}$ are none other that the mirror of primordial cosmological perturbations. The CMB, thanks to the properties of the Compton scattering, is linearly polarized and polarization represents a crucial additional information for cosmology. The CMB polarization anisotropies are usually not analysed in terms of Q and U Stokes parameters but via their combination E and B [2]. Different cosmological models have different predictions for CMB anisotropies in temperature and polarization and therefore the CMB is crucial to investigate and constrain the standard cosmological model and its extensions. In this paper we ill briefly review the main cosmological results by *Planck* 2015 [3, 4, 5, 6, 7, 8].

2 Planck 2015

The *Planck* mission[1] is the third generation of satellites dedicated to the observation of the sky in the microwaves. It is an ESA project and was launched on the 9th of May 2009 and has observed the sky continuosly from the 12th of August 2009 to the 23rd of October 2013 in 9 bands between 30 GHz and 1 THz, it has angular resolutions between 5 and 30 arcmin and a sensitivity of $\Delta T/T_{CMB} \sim 2 \times 10^{-6}$ [9]. The satellite is composed by two instruments based on two different detector technologies: the Low Frequency Instrument (LFI), composed by radiometers at 30, 44, 70 GHz that operated for about 48 months , and the High Frequency Instrument (HFI), composed by spider-web bolometers at 100, 143, 217, 353, 545 and 857 GHz that operated for about 30 months. The first data, and associated scientific results, release took place in 2013 [10] with the delivery of the first 15 months of temperature data. In 2015 there has been the second data and result release [3] with the full mission data in temperature and, for the first time, also in polarization. With respect to the 2013 release some changes have been made to the data, in particular, there has been a strong improvement in the calibration, bringing the agreement between *Planck* and WMAP to less than few tenths of percent, the effect of the feature at $\ell \sim 1800$ in 2013 data has been removed, plus there have been some changes in the data analysis tools like the likelihood and the foreground modelling inside the likelihood.

2.1 Maps

Planck has produced full sky maps at all nine frequencies in temperature and polarization [11, 12] . But the microwave sky is not only the CMB signal but it is the composition of CMB and all the astrophysical signals like the contamination by our Galaxy and by unresolved point sources, which are called foregrounds. In order to separate the different components of the sky and extract the CMB in temperature and polarization *Planck* has used four different component separation methods all giving very consistent CMB maps [4]. In Fig.1 we show the results of one of the method (SMICA) in temperature and polarization [2].

2.2 Power Spectra

To perform a statistical analyisis of the CMB anisotropies, they are expanded in spherical harmonics $\Delta T(\vec{x}, \hat{n}, \tau) = \sum_{l=1}^{\infty} \sum_{m=-l}^{l} a_{lm}(\vec{x}, \tau) Y_{m,l}(\hat{n})$. The angular power spectrum is then defined as $C_l = \frac{1}{(2l+1)} \Sigma_m \langle a_{lm}^* a_{lm} \rangle$. If the primordial fluctuations were Gaussian, the angular power spectrum would provide a complete description of the CMB anisotropies, whereas in case of non-Gaussianities, like are predicted in different cosmological models, higher statistical moments like the bispectrum and the trispectum may be different from zero. In Fig.2 we show the *Planck* angular power spectra in temperature and polarization. The spectra shown are the temperature TT autocorrelation, the E-mode autocorrelation EE, the temperature-E-mode cross-correlation TE. We show also the B-mode polarization which has been derived

---

[1]*Planck* (http://www.esa.int/Planck) is a project of the European Space Agency (ESA) with instruments provided by two scientific consortia funded by ESA member states and led by Principal Investigators from France and Italy, telescope reflectors provided through a collaboration between ESA and a scientific consortium led and funded by Denmark, and additional contributions from NASA (USA).

[2]Due to ongoing data analyisis at the time of the release the lowest multipoles $\ell < 30$ of the polarization map have been filtered out, for a recent update on the low-ℓ polarization see [13]
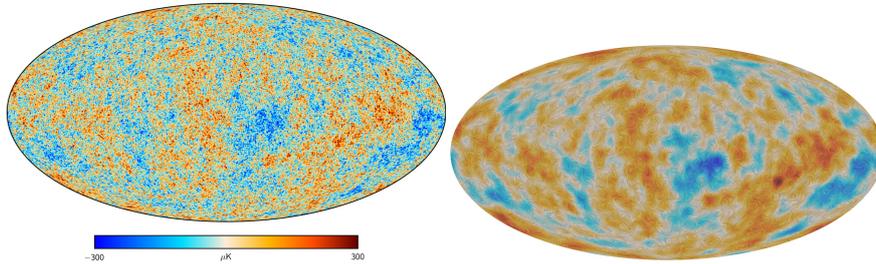
Figure 1: The component separated maps in temperature, left panel, and polarization, right panel.

with a joint analyisis of the *Planck* and BICEP-2/Keck data [14]. The B-mode polarization is particularly important since it is not produced by the standard density perturbations, i.e. scalar perturbations, apart from a late time contribution on small angular scale by the CMB gravitational lensing. Therefore large scale B-modes in the standard cosmological model are representative of tensor primordial perturbations and are considered the smoking gun of inflation, in fact their amplitude would be directly connected to the enegy scale of inflation [3].

2.3 Lensing

CMB photons travel almost unperturbed from the LSS, but during their crossing of the large scale structure they are subjected to the gravitational effects of the matter distribution in the Universe, the CMB lensing. The CMB lensing has distinctive signatures on the angular power spectra and it has a non-Gaussian contribution to the CMB anisotropies. The effect on the angular power spectra is a smoothing of the peaks in the temperature anisotropies, but most important, the lensing of the E-mode polarization generetes a non-zero B-mode polarization with a peculiar shape which peaks on small angular scales. This signal is crucial since it represents one of the main contaminants for the detection of the primordial B-mode polarization from inflation. Using the non-Gaussian contribution of the lensing to the CMB anisotropies *Planck* detected the lensing with a significance of more than 40 sigma and was able to extract the information on the lensing potential with unprecedented precision at the level of 2.5% accuracy [15]. It was also possible to reconstruct a full-sky map of the projected mass distribution. In Fig.3 we show the results of both the analyisis.

3 Cosmological Parameters

The *Planck* data are used to derive the constraints on the standard cosmological models and its extensions, exploring the cosmological parameter space using a a Markov Chain Monte Carlo approach, e.g. with the public code `CosmoMC` [16]. To derive the constraints presented in the next sections we used the *Planck* 2015 likelihood, which is described in detail in [5]. The *Planck* likelihood uses a hybrid approach with the combination of one likelihood dedicated to low-ℓ and

---

[3]Although there are other possible sources of B-modes connected with exotic cosmological models, like the one which includes primordial magnetic fields.
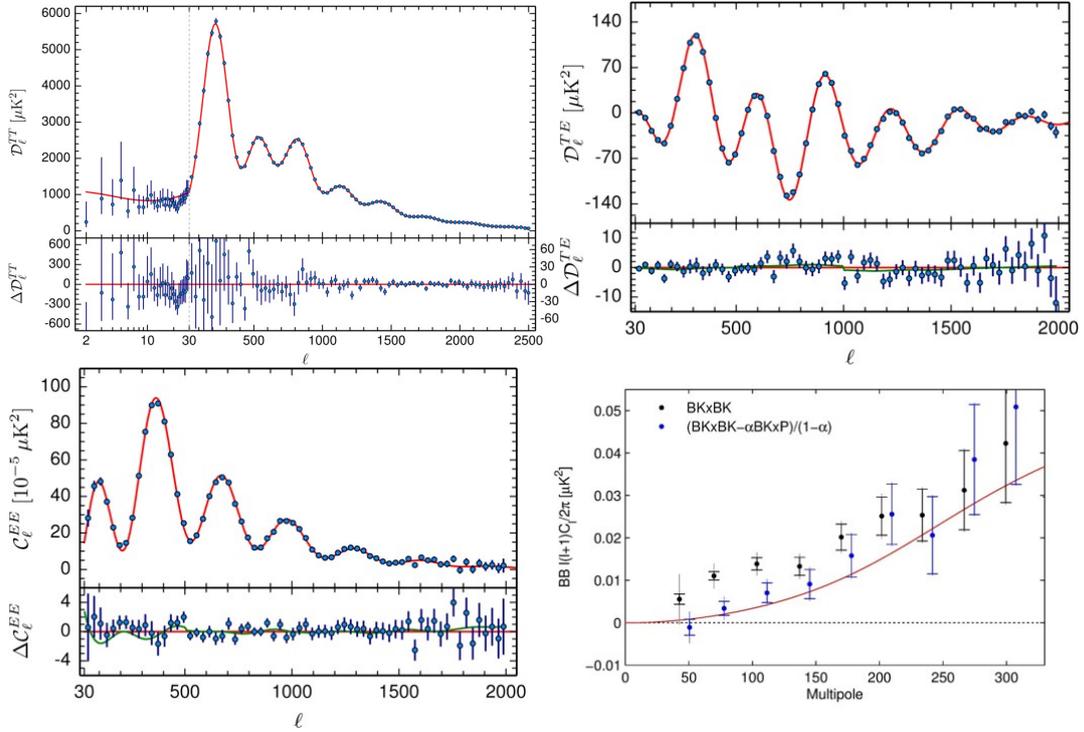
Figure 2: CMB anisotropy angular power spectra in temperature and polarization as measured by *Planck* 2015. The upper left panel is the temperature spectrum, the upper right is the temperature-E-mode cross-correlations, the lower left panel is the E-mode and the lower right panel is the joint analyisis of Planck and BICEP2/Keck of B-mode polarization.
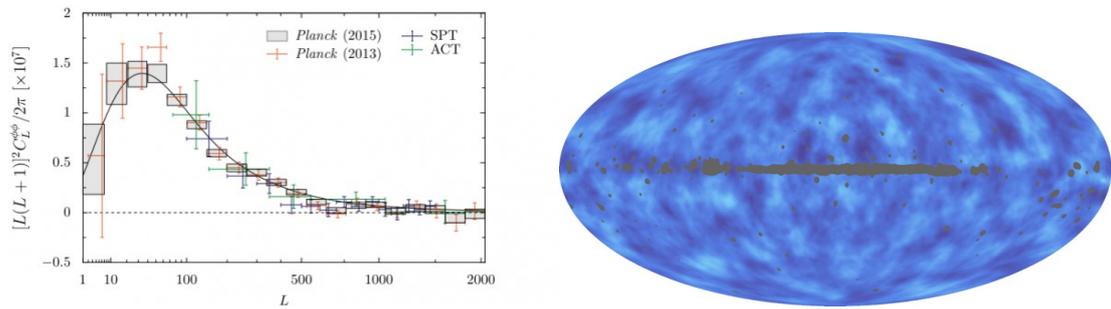
Figure 3: Planck 2015 lensing results, the lensing potential is on the left panel; the reconstructed matter distribution map on the right panel.

Parameter	TT+lowP	TT+lowP+lensing	TT,TE,EE+lowP	TT+lowP+lensing+ext
$\Omega_b h^2$	0.02222 ± 0.00023	0.02226 ± 0.00023	0.02225 ± 0.00016	0.02227 ± 0.00020
$\Omega_c h^2$	0.1197 ± 0.0022	0.1186 ± 0.0020	0.1198 ± 0.0015	0.01184 ± 0.0012
$100\theta_{MC}$	1.04085 ± 0.00047	1.04103 ± 0.00046	1.04077 ± 0.00032	1.04106 ± 0.00041
τ	0.078 ± 0.019	0.066 ± 0.016	0.079 ± 0.017	0.067 ± 0.013
$ln(10^{10}A_s)$	3.089 ± 0.036	3.062 ± 0.029	3.094 ± 0.034	3.064 ± 0.024
n_s	0.9655 ± 0.0062	0.9677 ± 0.0060	0.9645 ± 0.0049	0.9681 ± 0.0044
H_0	67.31 ± 0.96	67.81 ± 0.92	67.27 ± 0.66	67.90 ± 0.55

Table 1: Parameter 68% confidence limits for the base ΛCDM model from *Planck* CMB power spectra, in combination with lensing reconstruction ("lensing") and external data ("ext",i.e. BAO+JLA+H0)[6].

another to high-ℓ. The *Planck* low-ℓ likelihood is a fully pixel-based likelihood with temperature and polarization with an ℓ-range $2 < \ell < 29$ in TT, TE, EE, and BB. The likelihood is based on the foreground-cleaned LFI maps at $70\,\text{GHz}$ and the temperature map derived by the component separation method `Commander` [5]. This likelihood is denoted as *lowP* and is based entirely on *Planck* data for both temperature and polarization. The *Planck* high-ℓ likelihood is based on a Gaussian approximation and covers the ℓ-range $30 < \ell < 2500$. It uses the half-mission cross-power spectra of the $100\,\text{GHz}$, $143\,\text{GHz}$, and $217\,\text{GHz}$ channels. The likelihood takes foregrounds and secondary anisotropies into account [5]. It is denoted as *Planck TT*, for temperature only, or *Planck TT*, *TE*, *EE*, for temperature plus polarization. In addition to the likelihood based on the CMB anisotropies, the *Planck* collaboration has also delivered a likelihood based on the lensing potential with a conservative range in ell of $40 < \ell < 400$ [15]. In addition to the CMB based likelihood *Planck* uses also a compilation of other non-CMB datasets denoted as *ext* which include: BAO acoustic oscillationd from 6dFGS+SDSS+BOSS LOWZ; supernovae Ia ""Joint Light curve analysis from SNLS and SDSS, a prior on $H_0 = (73.9 \pm 3.3)$ Km/sec/Mpc, for details see [6].

3.1 ΛCDM

The standard cosmological model, the ΛCDM, is described by six cosmological parameters: the baryon density $\omega_b = \Omega_b h^2$, the cold dark matter density $\omega_c = \Omega_c h^2$, the reionization optical depth τ_{reion}, the ratio of the sound horizon to the angular diameter distance at decoupling θ, the scalar amplitude $\ln(A_s 10^{10})$, and the scalar slope n_s. The constraints derived with *Planck* 2015 likelihood are presented in Table 1. The ΛCDM is very well constrained and represents a very good fit to the *Planck* data.

3.2 Neutrinos

The baseline *Planck* model assumes a normal neutrino mass hierarchy with $\sum m_\nu = 0.06$ eV dominated by heaviest neutrino. The main effect of the mass of neutrinos is on large scale structure, the CMB is only slightly affected by neutrinos with masses below 1 eV. This is due to the fact that the effect of neutrino mass is caused by their transition from relativistic to non-relativistic, and becoming effectively an extra mass component for the CMB anisotropies, but this transition takes place well after recombination for masses below the eV. There is anyway
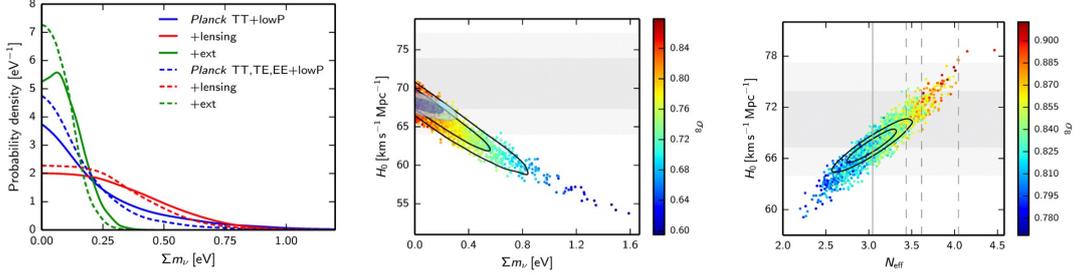
Figure 4: Constraints on neutrinos, on the first two panesl we shoe the posterior distribution of the sum of the masses and then the 2D joint distribution of the mass and the Hubble constant. On the third panel we show the 2D joint posterior for the number of effective neutrinos and the Hubble parameter.

an effect at recombination which affects the early Integrated Sachs Wolfe effect, caused by the changes in the gravitational potential wells induced by the transition. If not much can be said with CMB anisotropies, the lensing is instead strongly affected by neutrino mass, in fact massive neutrinos suppress the clustering of structures on scaler smaller than the horizon at the non-relativistic transition affecting the lensing potential. Therefore the lensing becomes a very powerful tool to constrain neutrino masses. In Fig.4 we show the results for the neutrino mass constraints. The 95% C.L. limits are $\sum m_\nu < 0.72$ eV for *Planck* TT+lowP; $\sum m_\nu < 0.21$ eV for *Planck* TT+lowP+BAO; $\sum m_\nu < 0.49$ eV for *Planck* TT,TE,EE+lowP; $\sum m_\nu < 0.17$ eV for *Planck* TT,TE,EE+lowP+BAO; $\sum m_\nu < 0.68$ eV for *Planck* TT+lowP+lensing; $\sum m_\nu < 0.59$ eV for *Planck* TT,TE,EE+lowP+lensing. The larger constraints with the addition of the lensing likelihood are due to the fact that the lensing likelihood based on the lensing potential reconstruction prefers lower values for the amplitude of the lensing signal with respect to the one derived with the CMB angular power spectra based likelihood and therefore the lensing likelihood allows for larger masses. Another possibility to investigate the neutrinos with CMB anisotropies are the constraints on the number of effective neutrinos. In fact, an increased number of effective neutrinos with respect to the standard prediction $N_{eff} = 3.046$ would lead to a faster expansion affecting both the Big Bang Nucleosynthesis predictions and the damping tail of the CMB anisotropies (it causes the recombination to happen earlier assuming the same size of the horizon as seen by Planck). The results are shown in the third panel of Fig.4. The *Planck* results are perfectly consistent with $N_{eff} = 3.046$ with single constraints given by (68% C.L.): $N_{eff} = 3.13 \pm 0.32$ *Planck* TT+LowP; $N_{eff} = 3.15 \pm 0.23$ *Planck* TT+LowP+BAO ; $N_{eff} = 2.99 \pm 0.20$ *Planck* TT,TE,EE+LowP; $N_{eff} = 3.04 \pm 0.18$ *Planck* TT,TE,EE+LowP+BAO. The constraints for the combination of variable mass and number of effective neutrinos confirms the results of the separate cases: $\sum m_\nu < 0.32$ eV and $N_{eff} = 3.2 \pm 0.5$ *Planck* TT+LowP+lensing+BAO. If we add a massive sterile neutrino in addition to the baseline three we have: $\sum m_\nu < 0.52$ eV and $N_{eff} < 3.7$ *Planck* TT+LowP+lensing+BAO and $\sum m_\nu < 0.38$ eV and $N_{eff} < 3.7$ *Planck* TT+LowP+lensing+BAO when restricting the prior on $m_{sterile}^{thermal} < 2$ eV instead of 10 eV of the first result.

3.3 Inflation

The inflation is a phase predicted in the standard cosmological model, in which the Universe underwent an exponential expansion [17]. Several models of inflation have been proposed through the years and each has its own predictions on the CMB anisotropies. Two of the main predictions of the most common inflationary models are a spectral index different from the scale invariance and the generation of tensor perturbations, therefore a tensor to scalar ratio r different from zero. In the left panel of Fig.5 we show the *Planck* 2015 and the combination of Planck+BICEP 2/KEck joint analysis results on the joint posterior distribution n_s and r compared with the predictions of some inflationary models. We note how *Planck* 2015, assuming a ΛCDM or ΛCDM+tensor model, excludes the scale invariance $n_s = 0.9655 \pm 0.0062$ (68% C.L.) with *Planck* TT+LowP, and gives strong upper limits on $r < 0.11$ *Planck* TT+LowP, reducing the allowed region of inflationary models [8].

3.4 Curvature, Dark Energy and Primordial Magnetic Fields

Two of the main extesions to the standard cosmological model consider models of dark energy which are not cosmological constants and the possibility to have non-zero curvature. In the first case *Planck* 2015 results are perfectly compatible with a dark energy in the form of a cosmological constant, this means that the parameter of the equation of state is $w = -1$. The *Planck* results on the dark energy are: $w = -1.54^{+0.62}_{-0.50}$ *Planck* TT+LowP; $w = -1.023^{+0.091}_{-0.096}$ *Planck* TT+LowP+ext; $w = -1.006^{+0.085}_{-0.091}$ *Planck* TT+LowP+lensing+ext; $w = -1.019^{+0.075}_{-0.080}$ *Planck* TT,TE,EE+LowP+lensing+ext. Also for the curvature *Planck* 2015 results are perfectly compatible with the standard cosmological model, namely with a flat geometry: $\Omega_k = -0.0512^{+0.049}_{-0.055}$ *Planck* TT+LowP;$\Omega_k = -0.040^{+0.038}_{-0.041}$ *Planck* TT,TE,EE+LowP;$\Omega_k = -0.005^{+0.016}_{-0.017}$ *Planck* TT+LowP+lensing;$\Omega_k = 0.0000 \pm 0.005$ *Planck* TT+LowP+lensing+BAO. The slight preference for negative values, closed universe, is due to a geometrical degeneracy and in fact note how adding the lensing and the BAO which break this degeneracy, brings the value in perfect compatibility with a flat geometry. The CMB allows to strongly constrain also more exotic cosmological models and in particular can give strong constrain to the one which considers the presence of primordial magnetic fields (PMF). PMF can naturally arise in the early Universe thanks to mechanisms related to inflation or phase transitions and may represent the progenitors of the fields we observe on large scale structures. PMF have several impact on CMB anisotropies [19, 18] and therefore CMB anisotropies can give strong constraints on PMF amplitude.*Planck* 2015 constraints are shown in the right panel Fig.5. The upper limits (95% C. L.) are: $B_{1Mpc} < 4.4$ nG *Planck* TT+lowP for generic spectral index; $B^{n_B=2}_{1Mpc} < 0.011$ nG; $B^{n_B=1}_{1Mpc} < 0.1$ nG; $B^{n_B=0}_{1Mpc} < 0.5$ nG; $B^{n_B=-1.5}_{1Mpc} < 4.8$ nG; $B^{n_B=-2.5}_{1Mpc} < 2.4$ nG; $B^{n_B=-2.9}_{1Mpc} < 2.0$ nG [7].

3.5 Conclusions

The *Planck* results represent a milestone in cosmology. The amount of data released is a legacy which will be exploited for years and years to come.*Planck* has confirmed that the ΛCDM model represents a very good fit to the CMB data, and has measured the cosmological parameters that describes it with unprecedented accuracy. But there are still a lot of challenges for the CMB future, the measurements of the B-mode polarization on large angular scales, the large scale anomalies etc. The final *Planck* release is expected for late 2016.
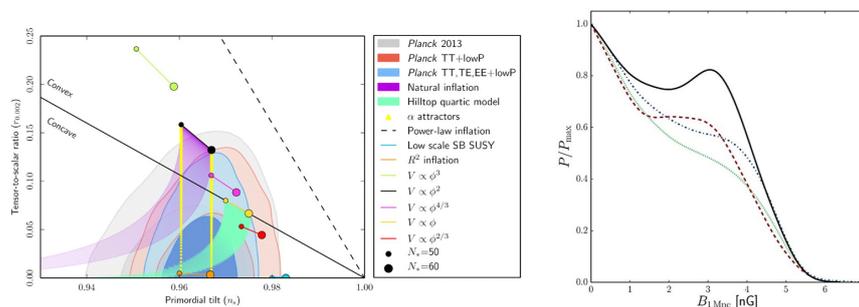
Figure 5: Constraints on inflation on the left and the constraints on primordial magnetic fields on the right: solid curve is Planck TT+lowP, compensated modes; the red dashed is Planck TT,TE,EE+lowP compensated; the green dotted line is PLanck TT+lowP compensated+passive modes; the blue dot-dashed is the Planck TT,TE,EE+lowP compensated+passive modes. .

4   Acknowledgments

References

[1] D. J. Fixsen, The Astrophys. J., **707**, 916 (2009).

[2] Hu W., White M., NewA, 2, 323 (1997).

[3] *Planck* Collaboration, arXiv:1502.01582 (2015).

[4] *Planck* Collaboration, arXiv:1502.05956 (2015).

[5] *Planck* Collaboration, arXiv:1507.02704 (2015).

[6] *Planck* Collaboration, arXiv:1502.01589 (2015).

[7] *Planck* Collaboration, et al., arXiv:1502.01594 (2015).

[8] *Planck* Collaboration, et al., arXiv:1502.02114 (2015).

[9] J.A. Tauber, N. Mandolesi, J.-L. Puget, et al. A&A, **520**, A1 (2010).

[10] *Planck* Collaboration, A&A, **571**, A1 (2014).

[11] *Planck* Collaboration, et al., arXiv:1502.01585 (2015).

[12] *Planck* Collaboration, et al., arXiv:1502.01587 (2015).

[13] *Planck* Collaboration, et al., arXiv:1605.02985 (2016).

[14] BICEP2/Keck and Planck Collaborations, Ade, P. A. R., Aghanim, N., et al., Physical Review Letters, 114, 101301,(2015).

[15] *Planck* Collaboration, et al., arXiv:1502.01591 (2015).

[16] Lewis A., Bridle S., ascl.soft, ascl:1106.025 (2011).

[17] Liddle A. R., Lyth D. H.,cils.book, 414 (2000).

[18] Paoletti D., Finelli F., 2011, PhRvD, 83, 123533

[19] Paoletti D., Finelli F., Paci F., 2009, MNRAS, 396, 523